

Predicting the Galvanomagnetic Coefficients of Tungsten from Fermi-Surface Data*

Jerome R. Long

Department of Physics, Virginia Polytechnic Institute and State University, Blacksburg, Virginia 24061

(Received 14 July 1970)

In the context of specific scattering processes, the galvanomagnetic coefficients of a metal crystal should be expressible in terms of features of the Fermi surface. For energy surfaces more complex than ellipsoids, however, analytical solutions of the transport equations with even the most tractable scattering assumptions have not been found, except in quadratures or in an asymptotic limit of the applied magnetic field. A procedure is introduced here for the purpose of predicting approximate values of arbitrary-field galvanomagnetic coefficients of a metal with nonellipsoidal Fermi-surface sheets. The procedure is based upon a semiempirical extension of the solution for ellipsoids. An application of the procedure to the Fermi surface of tungsten and measurements of the low-field galvanomagnetic coefficients of a tungsten crystal are described. The prediction is generally successful. No attempt is made to adjust parameters or obtain best fits to curves. The intent is to show how closely one can estimate by a simple, first-trial method.

INTRODUCTION

Certain transport effects, particularly the Hall effect and the magnetoresistance, are frequently treated as tools for investigating the Fermi surface of metals, with scant attention being given to transport processes *per se*.¹ Conversely, one frequently cited justification of Fermi-surface determinations is that transport properties of the electronic carriers in a nearly perfect large metal crystal can be derived from the shape of the Fermi surface. There are considerable mathematical difficulties, however, in solving a kinetic transport equation and current integrals for the complicated dispersion relations indicated by most Fermi surfaces. Only for ellipsoids and elastic scattering have reasonably complete results been obtained. A particularly compact and general treatment of the galvanomagnetic coefficients for ellipsoidal energy surfaces was given by Mackey and Sybert.² In the preceding paper,³ it was shown that there exists a simple geometrical interpretation of the Sondheimer-Wilson parameters⁴ which appear in the results of a Mackey-Sybert calculation of the magnetoconductivity tensor for tilted ellipsoids with anisotropic relaxation time. The implication is that the geometrical interpretation may apply to nonellipsoidal surfaces.

It is the purpose of this paper to apply the results of the preceding paper to the Fermi surface of tungsten. A semiempirical scheme is developed for obtaining, from Fermi-surface data, a quantitative estimate of the contribution of a given Fermi-surface sheet to the magnetotransport coefficients. The scheme appears to be restricted to cases where the magnetic field is applied along a symmetry axis of the crystal.

In a previous paper, the results of high-field measurements of six electrical and thermal trans-

port coefficients in a tungsten crystal were presented.⁵ The coefficients were measured in magnetic fields up to 22 kOe directed along a $\langle 100 \rangle$ axis at temperatures in the liquid-helium-4 range. Those data were obtained under high-field conditions (the product $\omega_c \tau$ of the cyclotron frequency and the phenomenological relaxation time is much greater than unity) and are not a very stringent test of the proposed scheme. In order to provide a better test, measurements of the magnetoresistivity and Hall resistivity of the same crystal were extended into the low-field ($\omega_c \tau < 1$) range. The semiempirical procedure was, thus, subjected to trial over a continuous field range from 5 Oe to 22 kOe.

Tungsten is an excellent metal for testing the proposed scheme. The major portions of the Fermi surface of tungsten are nonellipsoidal, with the electron "jack" having noncentral orbits,⁶ but the topology of its individual sheets is simple, there being no multiple connections or open orbits.

THEORY

The galvanomagnetic effects were measured in a tungsten crystal⁵ for which the electrical resistivity in zero magnetic field was found to be essentially independent of temperature at 4 K. It is thus assumed that electrical conduction in the crystal was limited by large-angle elastic scattering characterized by a relaxation time. The Sondheimer-Wilson theory⁴ as modified by Mackey and Sybert² would, therefore, be expected to be applicable to the galvanomagnetic effects in the crystal, were its Fermi-surface ellipsoidal, and any phenomena due to Landau quantization neglected. In that case, the magnetoconductivity $(\sigma_{11})_i$ and Hall conductivity $(\sigma_{12})_i$ due to the i th such ellipsoid or band of equivalent ellipsoids would be given in Gaussian units by^{3,5}

$$(\sigma_{11})_i = ecn_i a_i H_i / (H^2 + H_i^2), \quad (1a)$$

$$(\sigma_{12})_i = (\pm) ecn_i H / (H^2 + H_i^2). \quad (1b)$$

The quantities e , c , and H are the electronic charge, speed of light, and applied magnetic field. The i th band contains n_i carriers per cm^3 , which if hole- (electron-) like takes the $+$ ($-$) sign as indicated in Eq. (1b). H_i and a_i are defined from the point of view of the preceding paper.³ $H_i \equiv m_i^* c / e \tau_i^*$, where τ_i^* and m_i^* are the effective relaxation time and cyclotron mass of the i th band for the specified orientation of H . The geometrical definition of a_i is $a_i = (P_{\text{orb}}/P_{\text{cir}})^{1/2}$, where P_{orb} is the perimeter of the extremal orbit on the ellipsoid and P_{cir} is the perimeter of a circle which would enclose the same area (same de Haas-van Alphen frequency) as that enclosed by the extremal ellipse. The exponent ranges from the value 2 for isotropic scattering to 0 for scattering with the same anisotropy as the dispersion law.

The Sondheimer-Wilson theory assumes completely independent bands. This implies that the net conductivities of a multiband metal to which Eqs. (1) are applied are given by

$$\sigma_{11} = \sum_{\text{bands}} (\sigma_{11})_i \text{ and } \sigma_{12} = \sum_{\text{bands}} (\sigma_{12})_i.$$

EXPERIMENT

Extension of the galvanomagnetic data into the low-field range was accomplished with essentially the same apparatus and procedure as that used in measuring the high-field coefficients.⁵ Due to the small ($10^{-10} \Omega \text{ cm}$) magnitude of the resistivities in the low-field range, a few changes were necessary in order to make the measurements with the available conventional dc equipment.

All thermometers and heaters used in the thermal measurements were omitted, and instead of a single No. 36 strand, the electric current probe was made up of several parallel No. 30 strands in order to carry currents up to 10 A. Despite this modification and the immersion of the sample in liquid helium, significant Joule and Thomson heating were observed at the higher currents. This was apparently due to the insulating effect of bubbles formed in the helium I, particularly at the relatively high-resistivity conducting adhesive contacts⁵ between the strands of copper wire and the sample. Heating effects and the magnetoresistance due to the self-field of the sample current⁷ thus limited the maximum usable current density to about 90 A/cm^2 ($I \approx 7 \text{ A}$). Corrections for these extraneous effects were obtained by current reversal and by measuring the change in resistivity as a function of current in zero applied field.

The zero-field resistivity being nearly residual at 4.2 K, all of the measurements were performed

at this temperature for reasons of simplicity and economy. The heating effects could be reduced by working in helium II, but this did not allow higher current densities because of the self-field effect.

The advantages of enhancing the small signal by increasing the current density having been exhausted, the apparatus was further simplified by eliminating the six-dial potentiometer and feeding the voltage probes directly into a Keithly 148 nanovoltmeter mounted at the Dewar head. With repeated measurements, it was then possible to verify signal changes of less than one nanovolt. Each data point, Figs. 2 and 3, is an average of many trials, particularly at the lowest fields.

RESULTS

The kinetic coefficients σ_{11} and σ_{12} were computed from the measured magnetoresistivity ρ_{11} and Hall resistivity ρ_{21} through the usual inversion relations $\sigma_{11} = \rho_{11}/(\rho_{11}^2 + \rho_{21}^2)$ and $\sigma_{12} = \rho_{21}/(\rho_{11}^2 + \rho_{21}^2)$. In order to display both conductivities in the Lorentzian form indicated by Eqs. (1), the results are shown (Figs. 1 and 2) as the quantities $H\sigma_{11}$ and σ_{12} plotted against $\ln H$. The $H\sigma_{11}$ curve is seen to peak at about 85 Oe, while the σ_{12} data have a truncated peak centered at about 50 Oe and

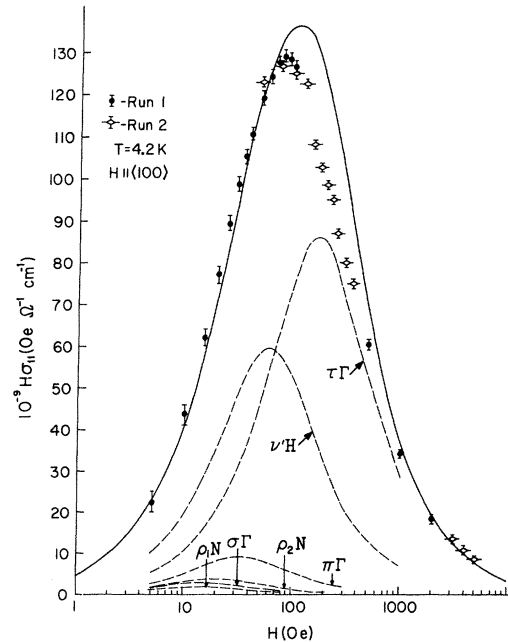


FIG. 1. Product of the applied magnetic field H and the transverse magnetoconductivity σ_{11} of the tungsten crystal plotted as a function of $\ln H$. Each broken, peaked curve was calculated [Eq. (1a)] from Fermi-surface data (Table I) and represents a band formed by a class of carriers on the Fermi surface. The unbroken curve, which approximately fits the data points, is the sum of the broken curves. Peak heights are proportional to $n_i a_i$.

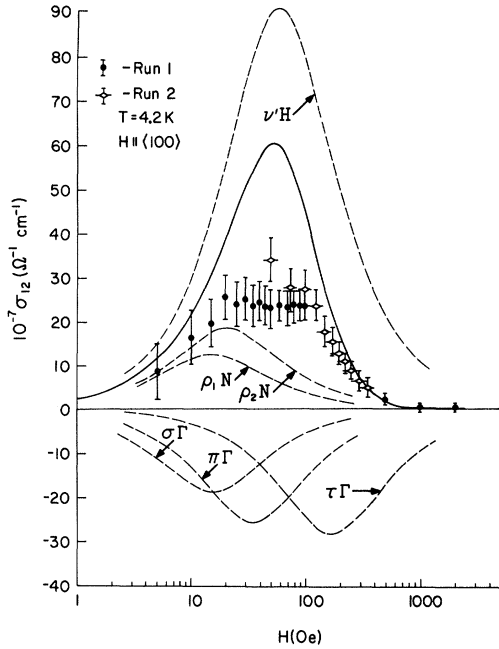


FIG. 2. Hall conductivity σ_{12} of the tungsten crystal plotted as a function of the natural logarithm of the applied magnetic field H . Each broken peaked curve was calculated [Eq. (1b)] from Fermi-surface data (Table I) and represents a band formed by a class of carriers on the Fermi surface. The unbroken curve is the algebraic sum of the broken curves. Peak heights are proportional to n_i/H_i .

are positive at all fields. The positions of the peaks tempt one to say that a "typical" carrier satisfies the condition $\omega_c\tau = 1$ somewhere in the field range 50–85 Oe. The band-by-band analysis

will show the limitations of such an estimate. The positive sign of σ_{12} at all fields is a clear indication that occupied hole states were in greater number, however slightly, and also more mobile than occupied electron states. This is consistent with the high-field data,⁵ which found $\sum_i (\pm)n_i > 0$, but $\sum_i (\pm)n_i H_i^2 < 0$.

The data points, Figs. 1 and 2, are approximated by an unbroken curve. The ordinates of each unbroken curve are the algebraic sums of the ordinates of the six broken curves. Each of the six broken curves was calculated from Eqs. (1). The parameters n_i , a_i , and H_i appearing in Eqs. (1) were determined, as will be discussed in the following section, by a procedure utilizing details of the tungsten Fermi surface constructed from de Haas-van Alphen data by Girvan, Gold, and Phillips⁶ (GGP), a model closely attuned to the theoretical work of Loucks⁸ and Mattheiss.⁹ The parameters are tabulated in Table I and specify a model of six independent bands.

ANALYSIS

The following semiempirical rule was developed for the purpose of selecting a portion of the k -space volume enclosed by a nonellipsoidal Fermi surface to be associated with a given i th band: When the magnetic field is directed along a given high-symmetry direction of the Brillouin zone, each class of extremal cyclotron orbit for that field direction may be associated with a distinct band. (Association of a band with an extremal orbit is supposedly justified for the transverse magnetic field transport effects upon the grounds that carriers in the vicinity of an extremal orbit are weighted heavily in the computation of the current, because they

TABLE I. Multiband parameters for $H \parallel (100)$. Sondheimer-Wilson parameters of the magnetoconductivity and Hall conductivity of a tungsten crystal calculated from experimentally determined details of the Fermi surface of tungsten. The parameters are defined by Eqs. (1) of the text.

i	Surface sheet	Orbit	m_i^*/m_0	H_i	H_i (Oe) for $H_0 = 170$ Oe	a_i	$n_i (10^{21} \text{ cm}^{-3})$	$a_i n_i H_i (10^{21} \text{ cm}^{-3})$	$a_i n_i H_i (10^{21} \text{ Oe cm}^{-3})$ for $H_0 = 170$ Oe
1	Hole ellipsoid	$\rho_1 N$	0.25	$0.25H_0/2.86$	14.8	1	0.234	$0.0204H_0$	3.47
2	Electron jack	$\sigma\Gamma$ neck	0.25	$0.25H_0/2.86$	14.8	1	0.35	$0.0304H_0$	5.17
3	Hole ellipsoid	$\rho_2 N$	0.35	$0.35H_0/2.86$	20.4	1.03	0.468	$0.0578H_0$	9.83
4	Electron jack	$\pi\Gamma$ knob	0.58	$0.58H_0/2.86$	34.5	1.05	1.1	$0.234H_0$	39.8
5	Hole octahedron	$\nu'H$	1	$H_0/2.86$	59.5	1.1	6.75	$2.595H_0$	441.5
6	Electron jack	$\tau\Gamma$ four ball	2.86	H_0	170	1.8	5.96	$10.72H_0$	1824
Sum							14.86	$13.65H_0$	2320

tend to have a large common velocity component in the direction of the applied electric field.) If a given sheet α of the Fermi surface has only a single central extremal orbit O_α for the chosen field direction, then the k -space volume of the band associated with O_α may be taken as the sum of the total volumes of all sheets within the reduced zone which are equivalent (in the applied field) to the α sheet. If a sheet β has multiple extremal orbits for the chosen field direction, then the k -space volume of the band associated with the j th orbit $O_{\beta j}$ may be taken as the sum of all volumes in the zone which are equivalent to the volume contained between a pair of planes that are parallel to the plane of the orbit, and pass through inflection points on the surface marking transitions from the contour of the j th extremal orbit to the $(j-1)$ th and $(j+1)$ th extremal orbits on the same sheet β of the Fermi surface.

Seven distinct classes of extremal area cyclotron orbit exist on the GGP surface when the magnetic field is directed along a $\langle 100 \rangle$ axis, the orientation used in the measurements reported here. The bands are denoted by a modified version of the orbit notation of GGP.

The hole Fermi surface includes six ellipsoids centered at the points N in the zone. Orbits on these ellipsoids are denoted by GGP as ρ . When the magnetic field is along $\langle 100 \rangle$, two of the ellipsoids have their long axis parallel to the field. A nearly circular orbit characterizes the band formed by these two ellipsoids. The band is denoted $\rho_1 N$, Fig. 3. The two remaining pairs of ellipsoids have their long axis normal to the field and display nearly identical elliptical orbits of nearly equal

cyclotron mass.¹⁰ It was assumed that a single band, denoted $\rho_2 N$ (Fig. 3), is formed by these two pairs of ellipsoids, thus reducing the number of independent bands from seven to six.

Most of the holes belong to the octahedron centered at the zone vertex H . The symbol ν was assigned by GGP to orbits on the octahedron. According to the extremal orbit criterion, the contribution of the hole octahedron to the data reported here should be characterized by the nearly square orbit (Fig. 3), which girdles the edges of the octahedron for $\vec{H} \parallel \langle 100 \rangle$. The notation $\nu' H$ has been assigned to this band to distinguish it from the $\langle 111 \rangle$ orbit denoted ν by GGP.

The $\langle 100 \rangle$ electron bands of tungsten are denoted by the symbols $\tau\Gamma$, $\pi\Gamma$, and $\sigma\Gamma$. These correspond to the orbits on the Γ -centered jack denoted τ , π , and σ by GGP. The τ orbit, also called the four-ball orbit, is central, while the π , or knob, and σ , or neck, orbits are both noncentral (Fig. 3).

Having apportioned the k -space volume enclosed by the Fermi surface into six bands, the carrier concentration n_i of each band (Table I) was simply given as the product $1/4\pi^3 \times (k\text{-space volume of the } i\text{th band})$.

Values of the coefficient a_i (Table I) depend on two sequential assumptions. The first of these was that the geometrical definition (perimeter rule) of a_i as derived for ellipsoids³ is applicable to a nonellipsoidal surface. Second, the exponent γ in the interpolation form of the perimeter rule was assumed to be unity. This choice seemed probable, since $0 \leq \gamma \leq 2$, and was the easiest to work with. One could use γ as a fitting parameter if he took the perimeter rule very seriously.

The method used to calculate the quantities $H_i = m_i^* c / e \tau_i^*$ of each of the six bands depended upon an assumption that the same effective relaxation time τ^* applied to all bands. There was no basis for this assumption other than computational simplicity, and ignorance of a better choice. Upon the assumption of a common τ^* , all of the H_i were scaled by means of effective mass data¹⁰ and expressed in terms of a single unknown. The unknown chosen was H_6 of the high-mass four-ball orbit $\tau\Gamma$ on the electron jack; then, $H_i = (m_i^* / m_6^*) H_6$.

From the prescription outlined above, it was possible to calculate the product $a_i n_i H_i$ for each band within the common factor H_6 ; then, $\sum_i a_i n_i H_i = 13.65 H_6 \times 10^{21} \text{ Oe cm}^{-3}$ (Table I). The factor H_6 depends upon τ^* , which is, at least, a function of the impurity concentration in a particular sample. At least one data point was, therefore, required. From high-field measurements⁵ on the same crystal, it was determined that $\sum_i a_i n_i H_i = 2.32 \times 10^{24} \text{ Oe cm}^{-3}$ in the context of Eqs. (1) for $H \gg H_i$. It was thus found that $H_6 = 170 \text{ Oe}$. A set of numbers was then available (Table I) which was used to

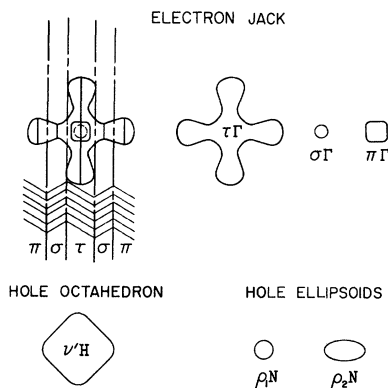


FIG. 3. Six distinct extremal cyclotron-orbit shapes on the Fermi surface of tungsten when a magnetic field is applied along a cubic axis. A conduction band is associated with each orbit in the calculation of the galvanomagnetic coefficients [Eqs. (1)]. The upper left view shows the partitioning of the volume of the electron jack into three volumes, corresponding to the π , σ , and τ orbits on the jack.

calculate the individual band and net behavior of $H\sigma_{11}$ and σ_{12} at all fields (Figs. 1 and 2).

DISCUSSION

The qualitative similarity between the predicted and measured behavior of $H\sigma_{11}$ (Fig. 1) is very satisfactory for such a simplified calculation. That the gross features of the weak-field coefficients and the strong-field coefficients are simultaneously consistent with Eqs. (1) should be well established by these results, since the position of the weak-field relaxation peak was set by the solution for H_6 as a force fit of $\sum_i a_i n_i H_i$ to the strong-field measurements. There is no support for the theoretical contention⁴ that the condition $\omega_c \tau \gg 1$ invalidates a description of the monotonic conductivities in terms of Eqs. (1) or other results based on a classical transport equation. At 22 kOe, the highest field utilized,⁵ $\omega_c \tau$ of the massive electrons on the $\tau\Gamma$ orbit reaches the value $H/H_6 \approx 130$.

The quantitative discrepancies between the predicted and measured behavior of $H\sigma_{11}$ can be understood somewhat by studying the predicted behavior of the individual bands (Fig. 1). Each band peaks at $H = H_i$, with the peak height being proportional to $a_i n_i$. Although there are six bands, it should be clear from Fig. 1 that $H\sigma_{11}$ is dominated by the $\nu'H$ and $\tau\Gamma$ bands and that only very drastic changes of any of the other four bands would produce a significant adjustment of the calculations. The most obvious adjustment is a reduction of H_6 by about $\frac{1}{3}$. A change in H_6 is reasonable, as there were never any theoretical grounds for the initial assumption of an equal relaxation time for all sheets of the Fermi surface, and the scattering dynamics of the τ orbit would appear to be significantly different from the dynamics of the other more nearly circular orbits. A simultaneous reduction of $a_6 n_6$ by about 20% is also indicated. Such a reduction would imply either a failure of the perimeter rule or of the method used for apportionment of the jack volume among its three extremal orbits.

The Hall conductivity (Fig. 2) is a much better test of the calculated parameters than $H\sigma_{11}$ because the calculated σ_{12} is a resultant of six terms of alternating sign and comparable magnitude, whereas $H\sigma_{11}$ is not sign sensitive and was dominated by only two bands. The peak heights of the individual bands in σ_{12} are proportional to n_i/H_i , so the assigned values of H_i are tested by both peak magnitude and position. The bands of high mobility are obviously weighted more heavily in σ_{12} than in $H\sigma_{11}$ and are more sensitive to the n_i assignments, without ambiguity due to a_i .

Agreement between the calculated resultant σ_{12} and data is thus remarkably good. The fit at low- and high-field extremes is good, and the qualita-

tively large overestimate of the peak height is no larger than the height of the least effective of the six bands. Furthermore, the σ_{12} results appear reasonably consistent with the $H\sigma_{11}$ results. In discussing $H\sigma_{11}$, a $\frac{1}{3}$ reduction of H_6 was suggested. The same adjustment in the σ_{12} calculation removes approximately half of the excess peak in the resultant σ_{12} . A reduction in the value of n_6 is not implied. The indicated 20% reduction of $a_6 n_6$ in the $H\sigma_{11}$ calculation would, therefore, come at the expense of a_6 , thus apparently weakening the perimeter rule.

Because the calculation of the H_i is seemingly in error, with a reduction of H_6 indicated, it is fortunate that a sensitive independent check of this calculation is available. From the field dependence of σ_{12} at high fields, the result $\sum_i (\pm) n_i H_i^2 = -3.86 \times 10^{26} \text{ cm}^{-3} \text{ Oe}^2$ was obtained.⁵ The calculated parameters of Table I yield a smaller number $-1.49 \times 10^{26} \text{ cm}^{-3} \text{ Oe}^2$. A reduction of H_6 is obviously inconsistent with the large experimental value of $\sum_i (\pm) n_i H_i^2$. An alternative adjustment of the parameters, which is more consistent with all of the data, would be to increase, rather than decrease, H_6 while simultaneously transferring many of the electrons from the four-ball $\tau\Gamma$ band to the $\sigma\Gamma$ band on the adjacent necks of the jack (Fig. 3). This alternative would also allow retention of the large value of a_6 calculated by the perimeter rule and tend to produce the shoulder which can be seen in the peak of the $H\sigma_{11}$ data at about 200 Oe.

The semiempirical calculation of the kinetic galvanomagnetic coefficients σ_{11} and σ_{12} having been more successful than expected, it was of interest to see how well the Table I transport parameters could predict the behavior of the thermoelectric coefficients measured at high fields.⁵ For fields $H \gg H_i$ the expressions equivalent to Eqs. (1) for kinetic thermoelectric coefficients ϵ''_{11} and ϵ''_{12} are

$$\epsilon''_{11} = \frac{\pi^2 k_B^2 c T}{3H^2} \sum_i (\pm) Z_i a_i H_i, \quad (2a)$$

$$\epsilon''_{12} = -\frac{\pi^2 k_B^2 c T}{3H} \sum_i Z_i, \quad (2b)$$

where all symbols are either standard or as defined for Eqs. (1), except Z_i which is the density of states of the i th band. The high-field measurements⁵ of ϵ''_{11} and ϵ''_{12} at approximately 4.2-K temperature were substituted into the above expressions to obtain the numbers $\sum_i Z_i = 2.3 \times 10^{34} \text{ erg}^{-1} \text{ cm}^{-3}$ and $\sum_i (\pm) Z_i a_i H_i = -3.6 \times 10^{37} \text{ erg}^{-1} \text{ cm}^{-3} \text{ Oe}$. In order to calculate these same quantities in terms of Table I parameters it was necessary to arrive at a set of numbers for the Z_i . These were estimated from Table I parameters in terms of the free-electron expression $Z_i = m_i^* (3\pi^2 n_i)^{1/3} (\pi \hbar)^{-2}$.

It was thus calculated that $\sum_i Z_i = 2.1 \times 10^{34} \text{ erg}^{-1} \text{ cm}^{-3}$ and $\sum_i (\pm) Z_i a_i H_i = -0.38 \times 10^{37} \text{ erg}^{-1} \text{ cm}^{-3} \text{ Oe}$. The calculated $\sum_i Z_i$ is as close as should be reasonably expected for a free-electron (band effective-mass approximation) calculation. It is, appropriately, less than the measured value which contains renormalization terms. The negative sign of $\sum_i (\pm) Z_i a_i H_i$ is a consequence of the large masses of the jack electrons on the four-ball orbit, which far exceeds the slight hole majority which gives σ_{12} its positive sign. The large ratio of measured to predicted $\sum_i Z_i a_i H_i$ is also understandable in terms of the H_i factor. It was seen in the high-field measurements⁵ that temperature-independent large-angle scattering was only dominant in the galvanomagnetic data and that the thermal effects were, apparently, controlled by a shorter and temperature-dependent relaxation time. A set of larger H_i than those in σ_{11} and σ_{12} should thus be expected to determine $\sum_i Z_i a_i H_i$. Equations (2) should not be expected to work very well when inelastic processes are significant.

CONCLUSIONS

The low-field magnetoconductivity and Hall conductivity for a transverse field applied along a

$\langle 100 \rangle$ axis of the tungsten crystal were calculated from high-field transport and de Haas-van Alphen data according to the proposed semiempirical prescription. The gross features of the calculated coefficients were found to be in good agreement with an experimental determination of the coefficients. It bears emphasizing that no attempt was made to adjust parameters or obtain a best fit to curves. The intent of Figs. 1 and 2 is to show how closely one can estimate by a simple first trial method. Discrepancies between data and calculation appear to have been principally due to failure of the assumption of a common relaxation time and errors in the apportionment of the k -space volume of the electron jack.

A definite evaluation of the methods used to apportion the carriers among a set of bands and to calculate the effect of the shape of the Fermi surface was not possible, but the results seem sufficiently encouraging to merit additional work for other field orientations and other metals. It is hoped that such results might serve to guide those who would attempt to obtain solutions of the transport equation. At the least, they may provide a simple rule of thumb for estimating the transport properties of the carriers in a given region of a Fermi surface.

*Experiments and preliminary analysis conducted in the Laboratory for Research on the Structure of Matter of the University of Pennsylvania with support by the Advanced Research Projects Agency of the U. S. Department of Defense under Contract No. SD-69. The work was completed at Virginia Polytechnic Institute with support by NASA.

¹E. Fawcett, *Advan. Phys.* **13**, 139 (1964).

²H. J. Mackey and J. R. Sybert, *Phys. Rev.* **180**, 678 (1969).

³J. R. Long, first preceding paper, *Phys. Rev. B* **3**, 1197 (1971) (Paper II).

⁴A. H. Wilson, *Theory of Metals* (Cambridge U. P., Cambridge, England, 1953), p. 208ff.

⁵J. R. Long, second preceding paper, *Phys. Rev. B* **3**, 1206 (1971) (Paper I).

⁶R. F. Girvan, A. V. Gold, and R. A. Philips, *J.*

Phys. Chem. Solids **29**, 1485 (1968). A good bibliography of the fermiology of tungsten may be assembled from the references in this paper. These authors refer to an extremal orbit as noncentral if the k -space coordinates of the orbit centers are not given by crystal symmetry.

⁷K. H. Berthel, *Phys. Status Solidi* **5**, 159 (1964).

⁸T. L. Loucks, *Phys. Rev.* **143**, 506 (1966).

⁹L. F. Mattheiss, *Phys. Rev.* **139**, A1893 (1965).

¹⁰W. M. Walsh, Jr., in *Resonances Both Temporal and Spatial*, edited by J. F. Cochran and R. R. Haering (Gordon and Breach, New York, 1969). This reference contains data on effective masses of tungsten as obtained by cyclotron resonance. When a choice was possible, the cyclotron resonance masses were chosen in preference to those obtained from de Haas-van Alphen temperature dependence. Agreement between the two methods is good.